



# Parameter extraction of solar cell using intelligent grey wolf optimizer

Akash Saxena<sup>1</sup> · Ashutosh Sharma<sup>1</sup> · Shalini Shekhawat<sup>2</sup>

Received: 6 November 2019 / Revised: 8 August 2020 / Accepted: 18 September 2020 / Published online: 11 October 2020  
© Springer-Verlag GmbH Germany, part of Springer Nature 2020

## Abstract

The focus of power producers has shifted from conventional energy sources to sustainable energy sources because of the depletion of fossil fuels and carbon emission causing global warming and climate change. Solar cells are the most prominent option to deal with these problems. The precise estimation of solar cell parameters is very much required before their installation to achieve high efficiency. In recent years applications of several optimization algorithms for parameter estimation of the solar cell have been addressed. Recently, intelligent grey wolf optimizer (IGWO), which is an advanced version of grey wolf optimizer (GWO) incorporating a sinusoidal truncated function as a bridging mechanism and opposition based learning has been introduced. The wide applicability of this variant has been examined over different conventional benchmark functions and on some real problems. This fact motivated authors to employ this variant on parameter extraction process. The main motivation behind the implementation of IGWO on solar cell parameter estimation process is the efficiency of this version to deal with complex optimization problems. To estimate the PV cell parameter values, measurement of voltage and current are considered at three important points. These are open circuit point, short circuit point and maximum power point, for two solar cell representative models i.e. single diode model and double diode model. Results of IGWO are compared with the results of other variants of GWO on these two models and for three films (Mono crystalline, poly crystalline and thin film). Results reveal that IGWO produces better results.

**Keywords** Photovoltaic module · Parameter estimation · Single and double diode model · IGWO algorithm

## List of symbols

PV cell	Photovoltaic cell
$R_{SE}$	Resistance of series
$R_{SH}$	Resistance of parallel
$\psi$	Ideality factor
$I_{dmc}$	Generated photocurrent
$I_{rsc}$	Reverse saturation current
$\psi_1$ & $\psi_2$	Ideality factor of first and second diode
$I_{rsc_1}$ & $I_{rsc_2}$	Reverse saturation current of first and second diode

$I_D$	Shockley diode equation
$q$	Electron charge
$k$	Boltzmann constant
T	Absolute temperature of diode junction (Kelvin)
$N_S$	Number of series cells
$V_{OC}$ & $I_{OC}$	Voltage and current at open circuit point
$V_{SC}$ & $I_{SC}$	Voltage and current at short circuit point
$V_{MPP}$ & $I_{MPP}$	Voltage and current at maximum power point
$\vec{K}$ & $\vec{M}$	Coefficient vector
$\vec{Y}$	Position vector of grey wolf
$r_1$ & $r_2$	Random numbers
$\vec{c}$	Control vector

✉ Akash Saxena  
akash@skit.ac.in

Ashutosh Sharma  
ashutoshsharma199566@gmail.com

Shalini Shekhawat  
drshalini@skit.ac.in

<sup>1</sup> Department of Electrical Engineering, Swami Keshvanand Institute of Technology, Management and Gramothan, Jaipur, India

<sup>2</sup> Department of Mathematics, Swami Keshvanand Institute of Technology, Management & Gramothan, Jaipur, India

## 1 Introduction

In present day scenario, many countries are trying to shift their focus from conventional sources of energy to renewable sources of energy because of limited availability and increasing cost of fossil fuels, environmental issues, global

warming and many others. Global warming and air pollution are major side effects of fossil fuels. According to research [1–6] several countries are now focusing on the use of renewable energy sources to a large extent to meet their increasing power demand and to protect environment. Generally, renewable energy is characterized as the energy which can be obtained from resources which can be replenished on their own. There are many renewable energy sources i.e. solar energy, hydro energy, wind energy, biomass energy, wave energy/marine currents and tidal energy. Sustainable energy sources are all depend on the direct or indirect utilization of solar energy. For future energy needs, the use of renewable energy sources are the only solution, as these are clean and cheap in comparison to non-renewable energy sources. Among all these sources, solar energy is very prominent non-conventional energy source due to its infinite availability, ease of installation, pollution and noise free nature [6, 7]. In the past years due to high initial cost and poor efficiency, solar energy could not be explored commercially. Through continuous research efforts the cost of solar cell has come down and it's efficiency has improved, hence it has drawn attraction of researchers for further research [7]. By using a device named as PV cell or solar cell, solar energy can be converted directly into electrical energy. There are numerous types of PV cells like amorphous silicon PV cell (a-Si), organic solar cell (OPV), bio-hybrid PV cell, cadmium telluride PV cell (CdTe), dye-sensitized solar cell (DSSC), concentrated PV cell (CVP and HCVP), copper indium gallium selenide solar cells (CI(G)S), photoelectrochemical cell (PEC), crystalline silicon solar cell (c-Si), gallium arsenide germanium solar cell (GaAs), hybrid solar cell, polycrystalline solar cell (multi-Si), thin-film solar cell (TFSC) etc [8].

To analyze the behavior of solar cells, different representative models have been studied. A few of them are single, double and triple diode models. By estimating the parameters of these representative circuits, a designer can easily analyze the behavior of these cells under different operating conditions. Hence, in this paper the parameter extraction using IGWO of single diode model and double diode model for three different cells i.e. thin-film, monocrystalline cell and polycrystalline cell have been carried out.

The reasons for selection of the above three types of PV cells to study effects of temperature and irradiance on them are discussed elsewhere [9, 10]:

- Solar irradiance and temperature vary throughout the day causing the efficiency of solar cell to vary. Whenever the solar irradiance increases, short circuit current and open circuit voltage also increase resulting in the shift of the maximum power point. To avoid this the position of solar cells can be rearranged according to the situation.

- Second factor, which affects the efficiency of solar cell is temperature. Photon production speed is boosted up as the temperature increases. This rapidly increases the reverse saturation current and by this band gap reduces. In this manner, this leads to marginal changes in current, but major changes in voltage.

Thus rise in temperature acts as a negative factor. To avoid this the position of solar cells can be rearranged according to the situation.

To construct a PV module, many PV cells are grouped together. Now researchers are focusing not only to reduce the cost of PV cells but also focus to enhance the reliability and efficacy of PV systems [11–14]. Among numerous numbers of existing models, researchers mainly used single and double diode model because complexity of the network increases exponentially increases as the number of diodes increase [15–17]. Single diode model is known for its fast convergence rate, simplicity and acceptable accuracy. Due to these reasons single diode model is commonly used model than others and also known as  $R_S$  or five parameter model. However, it has some limitations regarding to temperature variations. There are five parameters to extract in the single diode model i.e. ideality factor ( $\psi$ ), reverse saturation current ( $I_{rsc}$ ), photocurrent ( $I_{dmc}$ ), series resistance ( $R_{SE}$ ) and parallel resistance ( $R_{SH}$ ). In double diode model as one more diode is added making the network more complex. As one more diode is used in double diode model, loss in depletion region is occurred due to recombination of carriers [18]. In double diode model, there are seven parameters to be extracted i.e. diode ideality factor ( $\psi_1, \psi_2$ ), series resistance ( $R_{SE}$ ), shunt resistance ( $R_{SH}$ ), reverse saturation current of one diode ( $I_{rsc_1}$ ) and second diode ( $I_{rsc_2}$ ) and photovoltaic current ( $I_{dmc}$ ). Three diode model is also used where accuracy matters more over complexity. For this type of model, number of involved parameters increases upto 10. To find optimum circuit parameters of the PV device, transcendental equations are also required to relate I–V characteristic.

Utilization of metaheuristic algorithms for extraction of the representative models of solar panels have been addressed in past researches. Usually these approaches employ an objective function that is based on the minimization of the error of predicted and experimental values of current and voltage of PV panels at several data points. While exercising the optimal solutions different representative models can be utilised. In these approaches the fundamental data are not easily available at open and short circuit operating conditions, hence authors of [11] used a piece-wise I–V curve fitting method known as compound method to obtain differential values at these operating points. Authors of reference [19] extracted parameters of solar cell by using experimental IV characteristics of Si and Multi-junction solar cells. Authors presented comparative analysis of three different optimization

methods based on Newton-Raphson method and Levenberg-Marquardt algorithm and the last method was based on gradient search. Some of the optimization approaches like [19] are based on the initial guess and calculation of the gradient, hence a high probability is there when an optimization routine results in a local solution. To overcome this, multi point search solution techniques are employed. The application of Artificial Bee Colony (ABC) algorithm was explored by Diego Oliva et al. [20]. To extract parameters of solar panel Flower Pollination Algorithm (FPA) [21] was applied and explained nicely. Readers are further directed to the reference [15, 22] for reading the literature reviews on solar cell modelling and parameters estimation methods. The objective function given in [23] is used to minimize by a modified version of ABC algorithm which is highly effective version. The authors also compared the results with many other algorithms proving their algorithm much faster and accurate. Applications of Whale Optimization Algorithm (WOA) and its improved versions were explored in references [24, 25]. In these approaches opposition theory and different prey hunting mechanisms have been applied for enhancing the optimization capabilities of the WOA. Authors of [26] presented an objective function based on three important points and showcased that an approximate characteristics of PV panel can be obtained with the help of this analysis. Authors of this manuscript are motivated with the fact that these data are not abundant and practically not available for designers during the installation and commissioning of the panels. Further, the applications of metaheuristics in diverse fields such as in references [27–33] motivated authors to conduct this study with GWO improved variant.

In this paper, Intelligent Grey Wolf Optimizer (IGWO) is applied to solve parameter extraction process of solar panel by using two different representative models namely single diode and double diode models with three different films. The work is considered as an extension work of already published by Saxena et al. [34]. IGWO is a recently developed new variant of GWO. In IGWO, opposition based learning and a sinusoidal truncated function have been incorporated with conventional GWO to increase the search capability for better exploitation and exploration. With a sinusoidal truncated function, the search capability is increased and faster convergence can be achieved by using opposition based learning. With implementation of IGWO, it is possible to minimize the error sum in both single and double diode models. A comparison of IGWO with GWO and their variants is also presented in the paper. Fast convergence rate and optimality of the results are the main motivation behind the selection of IGWO compared to GWO.

After successful implementation of IGWO on some standard benchmark problems and a problem that is highly nonlinear and stochastic in nature as strategic bidding, authors are motivated to apply IGWO on parameter extraction process of

solar panel representative models. Following are the major research contributions of the manuscript:

1. An objective function that comprises of the error data points of short circuit, open circuit condition and maximum power point is evolved and modelled for three films and two representative models namely single diode and double diode models.
2. To compare various variants of GWO algorithm in extraction process of representative models and present analysis of the performance by exhibiting statistical attributes of the independent runs and convergence property analysis.
3. To compare the performance of the algorithms using different statistical analysis that includes paired t test, Wilcoxon rank-sum analysis and two sample t test and analyze the performance of the algorithm.

Remaining part of this manuscript is organized as follows: in Sect. 2 brief details of solar cell modelling and numerical data are presented, in Sect. 3 formulation of objective function is presented. Section 4 explains the details of native GWO and implementation steps of IGWO. In Sect. 5 results of the implementation of IGWO on solar cell parameter extraction process are explained and exhibited. The conclusion and future directions of the research work are shown in conclusion section.

## 2 Solar cell modelling and numerical data

It is very essential to understand a specific model which portrays the electrical conduct of solar cells. There are numerous proposed and developed equivalent circuit models out of which single diode model and double diode models are used commonly.

### 2.1 Single diode model

A single diode model is considered mostly due to its accuracy, fast convergence rate and simplicity (Figs. 1, 2, 3, 4).

Single diode model's I–V characteristic can be shown mathematically as [35]:

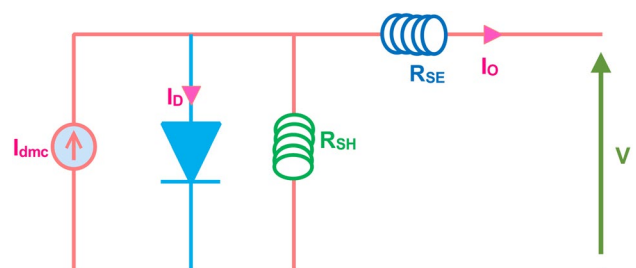


**Fig. 1** Representative equivalent circuit of PV module (single-diode model)

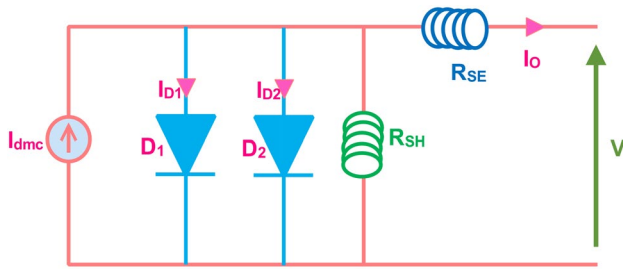


**Fig. 2** Representative equivalent circuit of PV module (double-diode model)

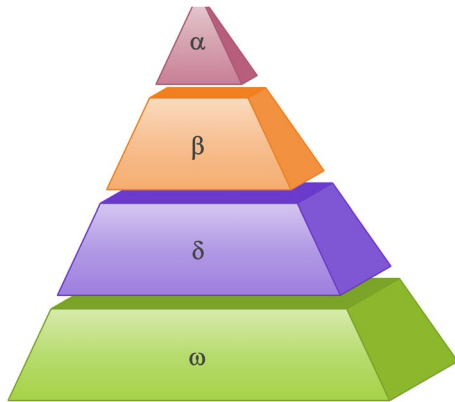


**Fig. 3** As per dominance upto down hierarchy of grey wolves

$$I_O = I_{dmc} - I_{rsc} \left[ \exp\left(\frac{q(V + I_O R_{SE})}{\psi k N_S T}\right) - 1 \right] - \left(\frac{V + I_O R_{SE}}{R_{SH}}\right) \tag{1}$$

For design and process of optimization, deep understanding of the parameters of PV cell is important. There are three cases at three crucial points:

**Case-1**  $V = V_{OC}$  and  $I_O = 0$  at open circuit point, then Eq. (1) reduces to:

$$I_{dmc} = I_{rsc} \left[ \exp\left(\frac{qV_{OC}}{\psi k N_S T}\right) - 1 \right] + \frac{V_{OC}}{R_{SH}} \tag{2}$$

**Case-2**  $V = 0$  and  $I_O = I_{SC}$  for short circuit point, then from Eq. (1) we get:

$$I_{dmc} = I_{SC} + I_{rsc} \left[ \exp\left(\frac{qR_{SE}I_{SC}}{\psi k N_S T}\right) - 1 \right] + \frac{R_{SE}I_{SC}}{R_{SH}} \tag{3}$$

from Eqs. (2) and (3), we get,

$$I_{rsc} = \frac{I_{SC} + \frac{R_{SE}I_{SC}}{R_{SH}} - \frac{V_{OC}}{R_{SH}}}{\exp\left(\frac{qV_{OC}}{\psi k N_S T}\right) - \exp\left(\frac{qR_{SE}I_{SC}}{\psi k N_S T}\right)} \tag{4}$$

Substituting Eqs. (4) into (2),

$$I_{dmc} = \frac{\left(I_{SC} + \frac{R_{SE}I_{SC}}{R_{SH}} - \frac{V_{OC}}{R_{SH}}\right) \left[\exp\left(\frac{qV_{OC}}{\psi k N_S T}\right) - 1\right]}{\exp\left(\frac{qV_{OC}}{\psi k N_S T}\right) - \exp\left(\frac{qR_{SE}I_{SC}}{\psi k N_S T}\right)} + \frac{V_{OC}}{R_{SH}} \tag{5}$$

**Case-3**  $V = V_{MPP}$  and  $I_O = I_{MPP}$  at Maximum Power point, Eq. (1) reduces in:

$$I_{MPP} = I_{dmc} - I_{rsc} \left[ \exp\left(\frac{q(V_{MPP} + R_{SE}I_{MPP})}{\psi k N_S T}\right) - 1 \right] - \frac{V_{MPP} + R_{SE}I_{MPP}}{R_{SH}} \tag{6}$$

### 2.2 Double diode model

By adding one more diode parallel to the existing diode is another model to show solar cell electrical conduct. Although it increases the network complexity but results in higher efficiency.

Mathematical representation of double diode model can be shown as:

$$I_O = I_{dmc} - I_{D1} - I_{D2} - \frac{V + I_O R_{SE}}{R_{SH}} \tag{7}$$

where  $I_{D1}$  and  $I_{D2}$  are shockley diode equations for first and second diode respectively, Eq. (7) can be rewritten as:

$$I_O = I_{dmc} - I_{rsc1} \left[ \exp\left(\frac{q(V + R_{SE}I_O)}{\psi_1 k N_S T}\right) - 1 \right] - I_{rsc2} \left[ \exp\left(\frac{q(V + R_{SE}I_O)}{\psi_2 k N_S T}\right) - 1 \right] - \frac{V + R_{SE}I_O}{R_{SE}} \tag{8}$$

Here we consider three cases at three crucial points which are:

**Case-1**  $V = V_{OC}$  and  $I_O = 0$  at open circuit point, then from Eq. (8) we can get:

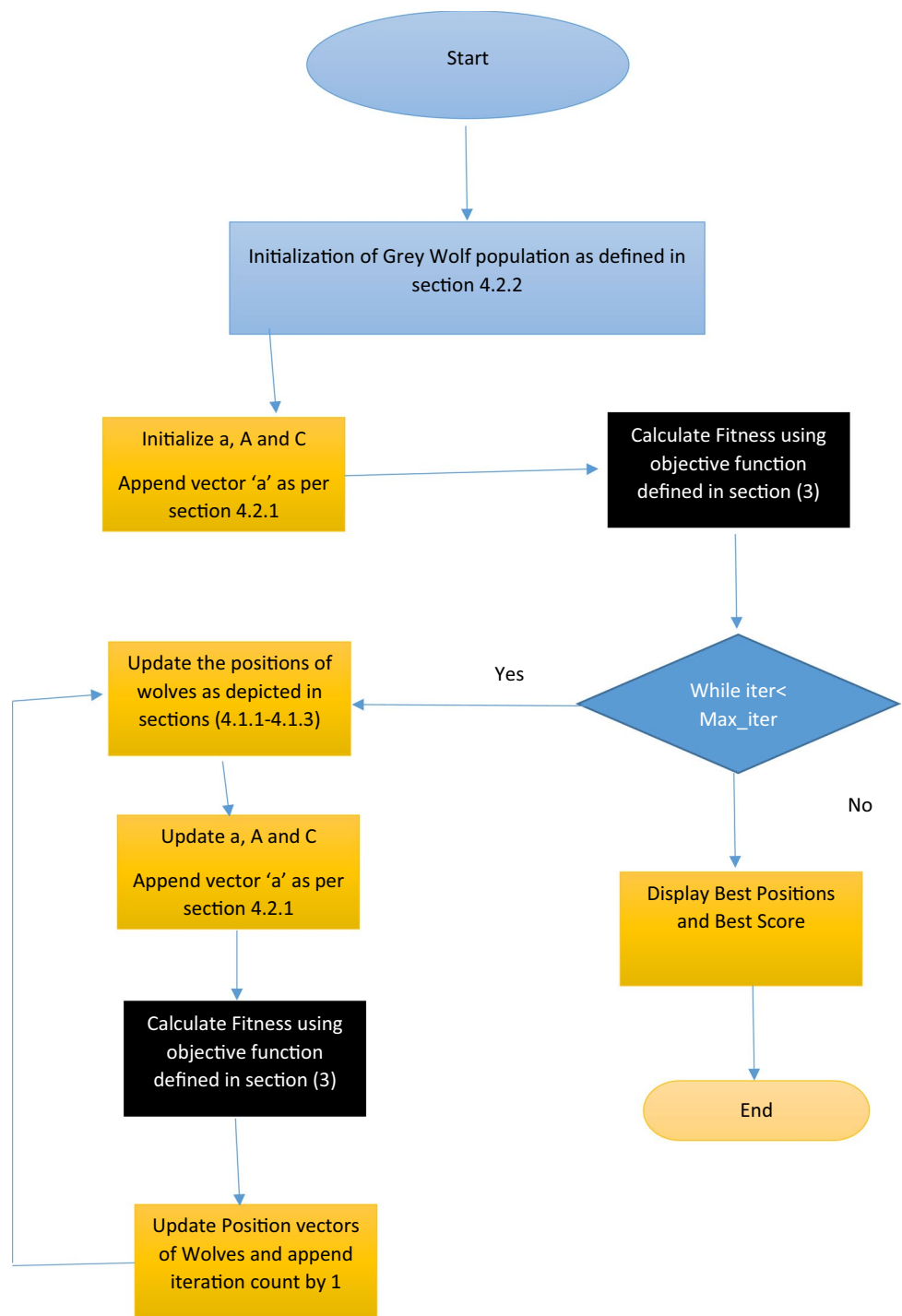
$$I_{dmc} = I_{rsc1} \left[ \exp\left(\frac{qV_{OC}}{\psi_1 k N_S T}\right) - 1 \right] + I_{rsc2} \left[ \exp\left(\frac{qV_{OC}}{\psi_2 k N_S T}\right) - 1 \right] + \frac{V_{OC}}{R_{SH}} \tag{9}$$

**Case-2** when  $V = 0$  and  $I_O = I_{SC}$  at short circuit point, therefore Eq. (8) can be rewritten as :

$$I_{dmc} = I_{SC} + I_{rsc1} \left[ \exp\left(\frac{qR_{SE}I_{SC}}{\psi_1 k N_S T}\right) - 1 \right] + I_{rsc2} \left[ \exp\left(\frac{qR_{SE}I_{SC}}{\psi_2 k N_S T}\right) - 1 \right] + \frac{R_{SE}I_{SC}}{R_{SH}} \tag{10}$$

from Eqs. (9) and (10) we find:

Fig. 4 Flow of IGWO



$$I_{rsc_2} = \frac{I_{SC} + \frac{R_{SE}I_{SC}}{R_{SH}} - \frac{V_{OC}}{R_{SH}} - I_{rsc_1} \left[ \exp\left(\frac{qV_{OC}}{\psi_1 k N_S T}\right) - \exp\left(\frac{qR_{SE}I_{SC}}{\psi_1 k N_S T}\right) \right]}{\exp\left(\frac{qV_{OC}}{\psi_2 k N_S T}\right) - \exp\left(\frac{qR_{SE}I_{SC}}{\psi_2 k N_S T}\right)} \quad (11)$$

substituting Eqs. (11) into (9):

$$I_{dmc} = I_{rsc_1} \left[ \exp\left(\frac{qV_{OC}}{\psi_1 k N_S T}\right) - 1 \right] + \frac{I_{SC} + \frac{R_{SE}I_{SC}}{R_{SH}} - \frac{V_{OC}}{R_{SH}} - I_{rsc_1} \left[ \exp\left(\frac{qV_{OC}}{\psi_1 k N_S T}\right) - \exp\left(\frac{qR_{SE}I_{SC}}{\psi_1 k N_S T}\right) \right]}{\left[ \exp\left(\frac{qV_{OC}}{\psi_2 k N_S T}\right) - \exp\left(\frac{qR_{SE}I_{SC}}{\psi_2 k N_S T}\right) \right] \left[ \exp\left(\frac{qV_{OC}}{\psi_2 k N_S T}\right) - 1 \right]^{-1}} + \frac{V_{OC}}{R_{SH}} \quad (12)$$

**Table 1** Electrical parameters for PV cells at standard test conditions

Type	Monocrystalline [36]	Polycrystalline [37]	Thin-film [36]
Number of cells in series, $N_s$	36	54	36
Temperature coefficient ( $I_{SC}, K_{I,SC}$ ) ( $\text{amp}^\circ\text{C}$ )	$0.8 \times 10^{-3}$	$3.18 \times 10^{-3}$	$0.35 \times 10^{-3}$
Temperature coefficient ( $V_{OC}, K_{V,OC}$ ) ( $\text{volt}^\circ\text{C}$ )	-0.0725	-0.123	-0.1
Voltage at maximum power point, $V_{MPP}$ (volt)	17.20	26.3	16.60
Current at maximum power point, $I_{MPP}$ (amp)	4.95	7.61	2.41
Open circuit voltage, $V_{OC}$	22.20	32.9	23.30
Short circuit current, $I_{SC}$	5.45	8.21	2.68

**Case-3**  $V = V_{MPP}$  and  $I_O = I_{MPP}$  at maximum power point, then from Eq. (8) we obtain:

$$I_{MPP} = I_{dmc} - I_{rsc_1} \left[ \exp\left(\frac{q(V_{MPP} + R_{SE}I_{MPP})}{\psi_1 k N_s T}\right) - 1 \right] - I_{rsc_2} \left[ \exp\left(\frac{q(V_{MPP} + R_{SE}I_{MPP})}{\psi_2 k N_s T}\right) - 1 \right] - \frac{V_{MPP} + R_{SE}I_{MPP}}{R_{SH}} \tag{13}$$

**2.3 Numerical data**

In this work, three types of solar cell modules i.e. monocrystalline, polycrystalline and thin-film are considered. Table 1 shows the typical data which is given by the designer. It is obvious to describe that at standard test condition of 1000 W/m<sup>2</sup> and 25 °C temperature, designer gives the data of voltage and current at three crucial points.

**3 Objective function**

The main objective of our optimization problem is to find out the values of different parameters of PV modules considered. These values must satisfied the standard values given in Table 1 at all the three crucial points. For single diode model three parameters are extracted through data-sheet information i.e.  $\psi$ ,  $R_{SE}$  and  $R_{SH}$ . Parameters  $I_{rsc}$  and  $I_{dmc}$  can be calculated from Eqs. (4) and (5) respectively. In double diode model five parameters i.e.  $\psi_1$ ,  $\psi_2$ ,  $R_{SE}$ ,  $R_{SH}$  and  $I_{rsc_1}$  are extracted and two parameters i.e.  $I_{rsc_2}$  and  $I_{dmc}$  can be calculated from Eqs. (11) and (12) respectively.

*Single diode model*

**Case-1** As depicted in Eq. (2) the error corresponds to open circuit is given by:

$$err_{OC} = I_{rsc} \left[ \exp\left(\frac{qV_{OC}}{\psi k N_s T}\right) - 1 \right] + \frac{V_{OC}}{R_{SH}} - I_{dmc} \tag{14}$$

**Case-2** As depicted in Eq. (3) the error corresponds to short circuit is given by:

$$err_{SC} = I_{SC} + I_{rsc} \left[ \exp\left(\frac{qR_{SE}I_{SC}}{\psi k N_s T}\right) - 1 \right] + \frac{R_{SE}I_{SC}}{R_{SH}} - I_{dmc} \tag{15}$$

**Case-3** As depicted in Eq. (3) the error corresponds to Maximum Power Point can be given by:

$$err_{MPP} = I_{dmc} - I_{rsc} \left[ \exp\left(\frac{q(V_{MPP} + R_{SE}I_{MPP})}{\psi k N_s T}\right) - 1 \right] - \frac{V_{MPP} + R_{SE}I_{MPP}}{R_{SH}} - I_{MPP} \tag{16}$$

*Double diode model*

**Case-1** As depicted in Eq. (9) the error corresponds to open circuit can be given by:

$$err_{OC} = I_{rsc_1} \left[ \exp\left(\frac{qV_{OC}}{\psi_1 k N_s T}\right) - 1 \right] + I_{rsc_2} \left[ \exp\left(\frac{qV_{OC}}{\psi_2 k N_s T}\right) - 1 \right] + \frac{V_{OC}}{R_{SH}} - I_{dmc} \tag{17}$$

**Case-2** From Eq. (10) short circuit point error is:

$$err_{SC} = I_{SC} + I_{rsc_1} \left[ \exp\left(\frac{qR_{SE}I_{SC}}{\psi_1 k N_s T}\right) - 1 \right] + I_{rsc_2} \left[ \exp\left(\frac{qR_{SE}I_{SC}}{\psi_2 k N_s T}\right) - 1 \right] + \frac{R_{SE}I_{SC}}{R_{SH}} - I_{dmc} \tag{18}$$

**Case-3** From Eq. (13) maximum power point error is:

$$err_{MPP} = I_{dmc} - I_{rsc_1} \left[ \exp\left(\frac{q(V_{MPP} + R_{SE}I_{MPP})}{\psi_1 k N_s T}\right) - 1 \right] - I_{rsc_2} \left[ \exp\left(\frac{q(V_{MPP} + R_{SE}I_{MPP})}{\psi_2 k N_s T}\right) - 1 \right] - \frac{V_{MPP} + R_{SE}I_{MPP}}{R_{SH}} - I_{MPP} \tag{19}$$

Now sum of the square of errors is taken as the main objective function for optimization.

$$ERR = err_{OC}^2 + err_{SC}^2 + err_{MPP}^2 \tag{20}$$

## 4 Brief overview of GWO and development of intelligent grey wolf optimizer (IGWO)

In this section, details of applied algorithm GWO and its recently developed variant IGWO are presented.

### 4.1 Grey wolf optimizer

It is a contemporary population-based swarm intelligence process. Mirjalili et al. [38] proposed this method, which is motivated by grey wolf behavior. In nature, grey wolves have the qualities of hunting mechanism and leadership hierarchy and GWO imitates these advantages. Grey wolves belong to canidae family. Usually, on an average 5-12 members of grey wolves prefer to live in a group. The wolves are classified in four categories: Alpha wolves are the dominant wolves in all four categories and are also the decision makers. After alpha wolves, beta wolves come in second position as per their dominance. Beta wolves are used to assist alpha wolves in decision making or in other activities of group. The order given by the alpha and beta wolves are followed by the delta wolves. In the hierarchy, the last position is occupied by omega wolves. They play role of scapegoat in wolf pack. Some applications of GWO have been covered in references [39–41]

The important procedures elaborated in the algorithm are as follows:

#### 4.1.1 Encircling the prey

Mathematical representation of the prey encircled by the grey wolves can be given as:

$$\vec{N} = |\vec{M} \cdot \vec{Y}_p(t) - \vec{Y}(t)| \tag{21}$$

$$\vec{Y}(t + 1) = \vec{Y}_p(t) - \vec{K} \cdot \vec{N} \tag{22}$$

where current iteration is represented by  $t$ ,  $\vec{Y}$  is position vector of grey wolf, coefficient vectors are  $\vec{K}$  and  $\vec{M}$ , and  $\vec{Y}_p$  is the position vector of the prey. We can calculate the vectors  $\vec{K}$  and  $\vec{M}$  as follows:

$$\vec{K} = 2\vec{c} \cdot \vec{r}_1 - \vec{c} \tag{23}$$

$$\vec{M} = 2 \cdot \vec{r}_2 \tag{24}$$

where control vector  $\vec{c}$  decreases linearly from 2 to 0 and  $r_1$  and  $r_2$  are the random numbers.

#### 4.1.2 Hunting the prey

It is not possible to find proper location of prey in the search space. Hence, to require the social hierarchy three best

solutions ( $\alpha, \beta$  &  $\delta$ ) are kept. This fact can be visualized by following mathematical equations :

$$\vec{N}_\alpha = |\vec{M}_1 \vec{Y}_\alpha - \vec{Y}|, \quad \vec{N}_\beta = |\vec{M}_2 \vec{Y}_\beta - \vec{Y}|, \quad \vec{N}_\delta = |\vec{M}_3 \vec{Y}_\delta - \vec{Y}| \tag{25}$$

$$\vec{Y}_x = \vec{Y}_\alpha - \vec{A}_x \cdot (\vec{D}_\alpha), \quad \vec{Y}_y = \vec{Y}_\beta - \vec{A}_y \cdot (\vec{D}_\beta), \quad \vec{Y}_z = \vec{Y}_\delta - \vec{A}_z \cdot (\vec{D}_\delta) \tag{26}$$

$$\vec{Y}_{(t+1)} = \frac{(\vec{Y}_x + \vec{Y}_y + \vec{Y}_z)}{3} \tag{27}$$

According to alpha wolves above equations represent position updation, where the distances of the prey are  $\vec{N}_\alpha, \vec{N}_\beta$  and  $\vec{N}_\delta$  from  $\alpha, \beta$  and  $\delta$  wolves respectively and positions of  $\alpha, \beta$  and  $\delta$  wolves are  $\vec{Y}_x, \vec{Y}_y$  and  $\vec{Y}_z$  respectively.

#### 4.1.3 Attacking prey

Accountability of this stage is for exploitation and it can be controlled by linear decrement in  $\vec{c}$ . Grey wolves are empowered by using linear decrement in  $\vec{c}$  to assault the prey, while it stops moving. By changing  $\vec{c}$  we can control the fluctuations in  $\vec{K}$  i.e. there are more fluctuations in  $\vec{K}$  if the value of  $\vec{c}$  is higher.

### 4.2 IGWO

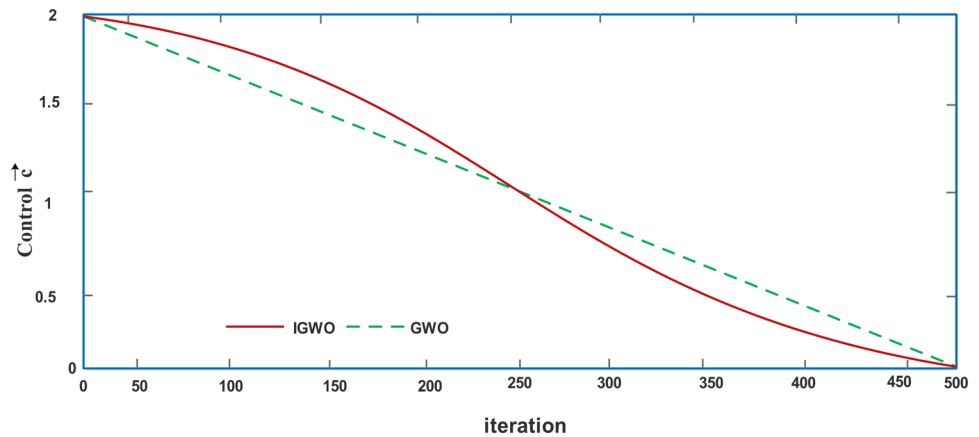
IGWO is a recently developed variant of GWO [34]. To increase the search capacity two modifications have been applied for superior exploration and exploitation. The first one is for better exploitation and exploration, in which control parameter is incorporated by using the sinusoidal truncated function. In the second modification, opposition based learning is used to provide better exploration.

#### 4.2.1 Control vector updation

In IGWO, direction and position control parameter  $\vec{c}$  is varied as a truncated sinusoidal function rather than to decrease linearly as per Eqs. (28) and (29). Grey wolves quit moving after hunting, this action is imitated by linear decrement in  $\vec{c}$ . During hunting, the values of  $\vec{c}$  are higher in first half where as in second half values of  $\vec{c}$  decrease very rapidly as compared with the classical GWO which is shown in Fig. 5. With the higher values of  $\vec{c}$  the search capability increases during hunting and it mimics the following behavior more efficiently.

$$\kappa = \pi \times \frac{\text{Current Iteration}}{\text{Maximum Iteration}} \tag{28}$$

**Fig. 5** By using sinusoidal truncated function variation of control parameter



$$c = 2 \times \left[ 1 - \sin^2 \left( \frac{\pi}{2} \right) \right] \tag{29}$$

### 4.2.2 Opposition based learning

In optimization methods, search starts from some initial guess or from a random point. If the initial point is near to the optimal solution then convergence can be achieved faster. On the other hand, if the chosen initial point is far away from the optimal location the convergence takes more time. Hamid R. Tizoosh introduced an opposition based learning approach in 2005 [42]. The search for the solution is done in every direction simultaneously. The basic concepts of opposition based learning are stated below:

**Definition 1** Let a real number is  $y \in [a, b]$ , then the opposite number of  $y$  is defined by:

$$\bar{y} = a + b - y \tag{30}$$

**Definition 2** Let a point in  $Q$  dimensional space is  $A = (y_1, y_2, \dots, y_Q)$ , where  $y_i \in \mathbb{R}, \forall i \in \{1, 2, \dots, Q\}$  and bounded by  $[a, b]$ , the opposite points matrix can be given by  $\bar{A} = [\bar{y}_1, \bar{y}_2, \bar{y}_3, \dots, \bar{y}_Q]$ . Hence

$$\bar{y}_i = [a_i + b_i - y_i] \tag{31}$$

### 4.3 Discussion

Unlike previous published approaches on GWO, the variant IGWO show cases the importance of bridging mechanism between the exploration and exploitation phase. The similar researches have been carried in references [43, 44]. However, a chaotic mechanism has been proposed by the authors in [45]. These algorithms have successfully showcased the impact of proper bridging between exploration and

exploitation phases. Along with this, implication of opposition theory has also been showcased in [46]. These examples are sufficient scientific proof that an adaptive bridging between diversification and intensification phases and some initial population diversification through opposition based learning can substantially enhance the optimization virtues of algorithm.

## 5 Results

In this section, simulation results for three different solar cells are analyzed with the application of IGWO algorithm. Both single and double diode models are running 30 times autonomously in this contextual study. Performance of IGWO is compared with other variants of GWO namely Modified Grey Wolf Optimizer (MGWO) [47], Grouped Grey Wolf Optimizer (GGWO) [48], Improved modified Grey Wolf Optimizer (ImGWO) [49], Modified Grey Wolf Optimizer (mGWO) [50] and Oppositional based Grey Wolf Optimizer (OGWO) [51].

### 5.1 Results for single diode model

The single diode model is simulated for extraction of parameters. For fair comparison, values of maximum iterations and search agents are kept same in all optimization techniques. Three parameters ( $R_{SE}, R_{SH}$  and  $\psi$ ) are extracted by using the algorithm, while the rest two parameters ( $I_{dmc}$  and  $I_{rsc}$ ) are calculated from the mathematical relation they share with the extracted parameters. The convergence curve of IGWO and the variants of GWO for monocrystalline cell are shown in Fig. 6, which shows the behavior of the algorithm. From this figure it can be concluded that IGWO converge faster than other algorithms. The parameter values extracted for monocrystalline cell, polycrystalline cell and thin films are shown in Table 2. The error analysis is depicted in Table 4 in terms of its mean, standard deviation, minimum (best)



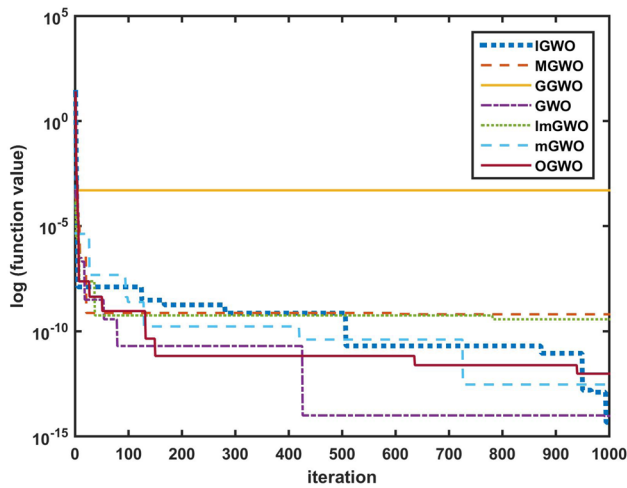


**Fig. 6** Convergence curve of monocrystalline-film by single diode model

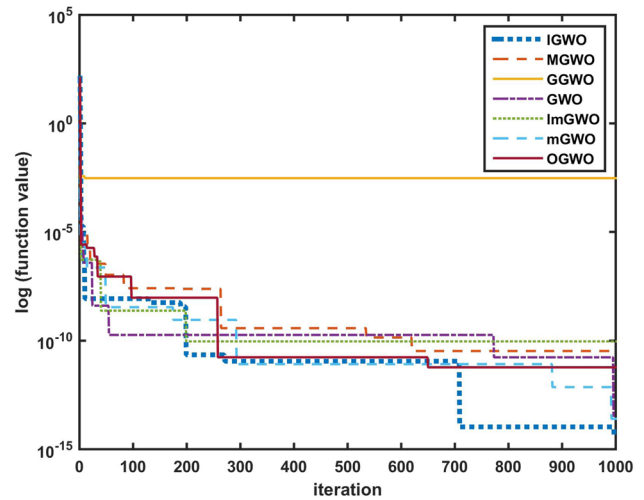


**Fig. 8** Convergence curve of polycrystalline-film by single diode model

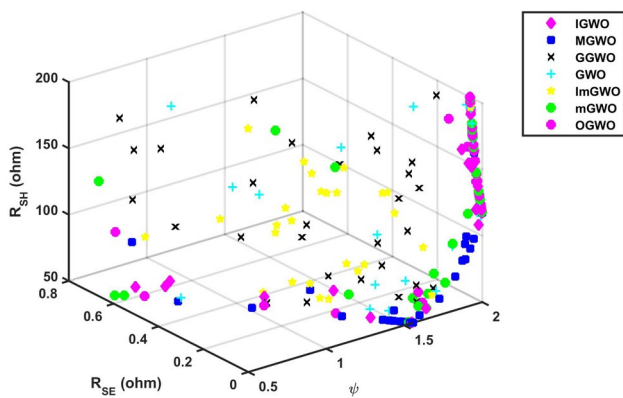


**Fig. 7** Scatter diagram using various algorithm for single-diode model of monocrystalline cell

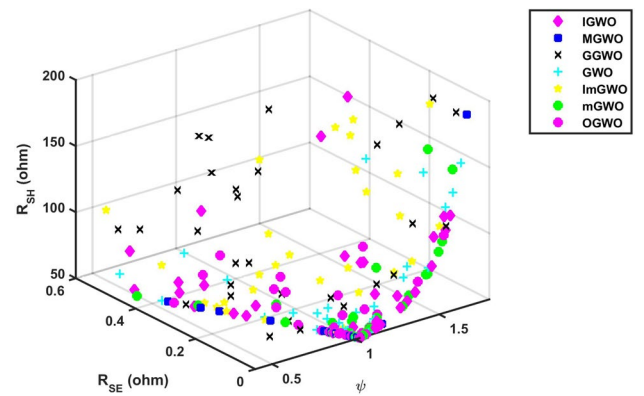


**Fig. 9** Scatter diagram using various algorithm for single-diode model of polycrystalline cell

and maximum (worst) values, which are obtained from the optimization process. The mean value of error obtained from IGWO drops down to  $10^{-15}$  which is the best obtained result as compared to other variants and the standard deviation values are also optimal which is clear from Table 4. Low value of standard deviation which is a good indicator shows better solution quality. The scatter diagram shows that the parameter values shifts over a reasonably wide range. The scatter diagram of the optimal solutions for 30 run of these parameters is shown in Fig. 7. The scatter plot is pairs of numerical data, with one variable along each axis, to look for a relationship between them and if the variables are correlated, the points will fall along a line or curve.

The same optimization study is carried out for polycrystalline and thin film solar cells. The results of both polycrystalline and thin film cells are obtained under similar conditions as applied on monocrystalline PV cell. The convergence curve of polycrystalline solar cell is shown in Fig. 8 and the scatter of

the optimal solutions of all the algorithms are shown in Fig. 9. The mean value of polycrystalline solar cell is  $8.5081E - 12$  and the value of standard deviation is  $4.2902E - 11$  which are optimal for IGWO according to Table 4. The optimal values are shown in boldface. The convergence curve and scatter diagram of thin film PV cell are represented in Figs. 11 and 12 respectively. The optimal mean value of thin film is  $7.0430E - 15$  and standard deviation is also the best for IGWO. The I–V characteristics of single diode model for all three films are shown in Fig. 10, which describe that these I–V characteristics satisfy the standard test conditions.

### 5.2 Double diode model

In double diode model, five parameters ( $\psi_1$ ,  $\psi_2$ ,  $SE$ ,  $R_{SH}$  and  $I_{rsc1}$ ) are extracted by using IGWO algorithm and the rest two parameters ( $I_{rsc2}$  and  $I_{dmc}$ ) are determined by the

**Fig. 10** I–V characteristics for **a** monocrystalline cell **b** polycrystalline cell, **c** Thin-film of Single diode model

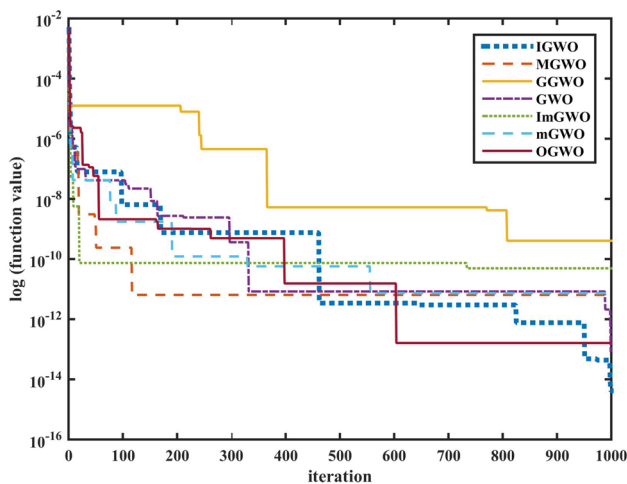
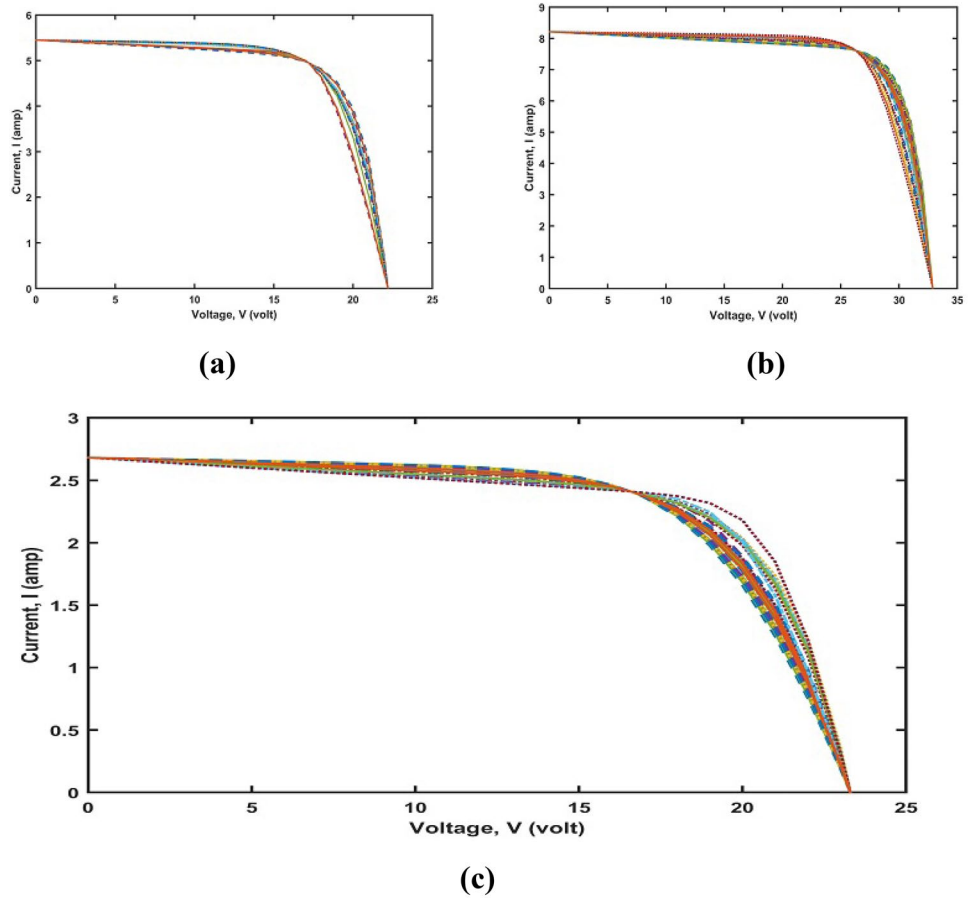


**Fig. 11** Convergence curve for thin-film by single diode model

mathematical relations, they share with the extracted parameters. The parameters obtained for all three PV cells i.e. monocrystalline, polycrystalline and thin-film are given in Table 3. Table 4 represents the comparison of error analysis of IGWO with other variants of GWO. The mean and SD values are not the best in case of monocrystalline cell but

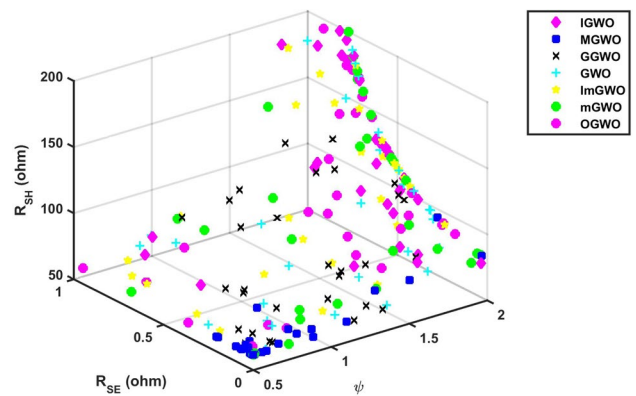


**Fig. 12** Single diode model’s scatter diagram using various algorithm of thin-film cell

these are not far from those obtained for the optimal solution. The convergence curve of monocrystalline solar cell is shown in Fig. 13 which depicts the behavior of IGWO in comparison with other GWO variants.

Similarly, the optimization performance is studied on polycrystalline and thin-film solar cell. The mean and standard deviation values of polycrystalline PV cells show optimal solution but for thin film mean and standard

**Table 2** Parameters values for single diode model

Algorithms	Monocrystalline solar cell						Polycrystalline solar cell						Thin-film					
	$\psi$	$R_{SE}$	$R_{SH}$	$I_{rsc}$	$I_{dmc}$	$I_{psc}$	$\psi$	$R_{SE}$	$R_{SH}$	$I_{rsc}$	$I_{dmc}$	$I_{psc}$	$\psi$	$R_{SE}$	$R_{SH}$	$I_{rsc}$	$I_{dmc}$	
IGWO	1.772027	0.100011	124.6638	2.32E-05	5.4581	1.087309	0.154975	79.9117	2.71E-07	8.229398	1.801296	0.584147	121.3472	4.90E-06	2.693835			
MGWO	1.57019	0.078241	67.66396	6.83E-06	5.457172	0.990683	0.054598	55.01213	1.79E-07	8.21896	0.77224	0.072707	63.69342	5.64E-07	2.682984			
GGWO	1.377377	0.286084	116.5616	2.04E-06	5.463912	1.009164	0.247184	107.0295	3.76E-07	8.232502	1.318245	0.427867	77.80583	9.14E-07	2.694079			
ImGWO	1.428793	0.261554	110.3373	4.00E-06	5.464907	1.076065	0.193585	96.68792	1.77E-07	8.230422	1.586979	0.574221	103.6401	3.83E-06	2.696139			
mGWO	1.712853	0.11888	119.5496	1.83E-05	5.458071	1.105049	0.01258	53.57058	3.64E-09	8.211928	1.577379	0.454528	102.3878	3.99E-06	2.691785			
OGWO	1.829613	0.090446	140.7862	2.56E-05	5.456333	1.03111	0.097636	59.50796	6.37E-08	8.223166	1.601251	0.523507	105.3417	3.94E-06	2.694159			
GWO	1.748881	0.123443	138.2758	1.93E-05	5.456436	1.095947	0.106395	73.34252	3.69E-07	8.224308	1.545721	0.463017	97.40618	3.63E-06	2.693356			

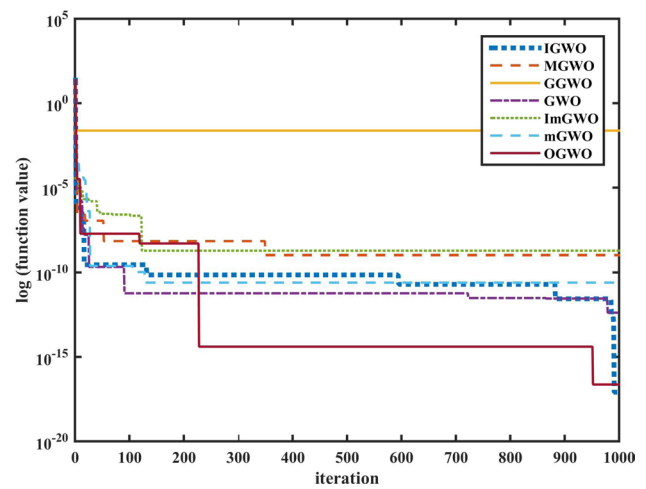


**Fig. 13** Monocrystalline film result comparison of double diode model

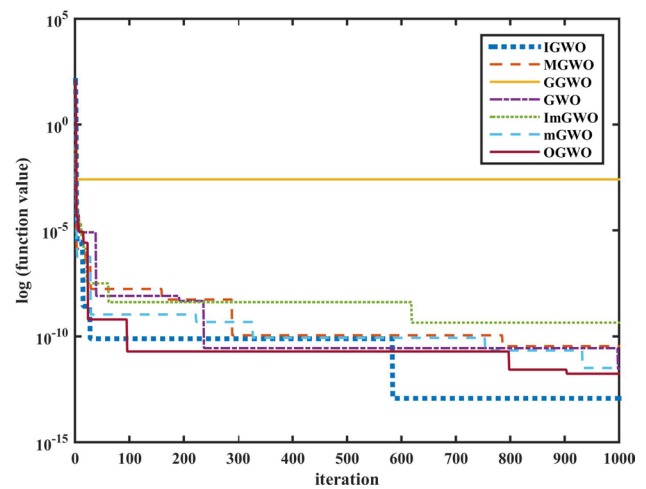


**Fig. 14** Polycrystalline convergence curve result comparison of double diode

deviation values are not optimal. These values are not very far from those obtained for optimal solution which shows that IGWO handles optimization satisfactorily. The convergence curve for polycrystalline cell is shown in Fig. 14 which shows that the convergence rate of IGWO is much better than other algorithms. For thin film, convergence curve is shown in Fig. 15. The mean and standard deviation values are at acceptable level compared to other algorithms. The I–V characteristics of double diode model are shown in Fig. 16 for all three films.

This study can be summarized by the following points:

1. Single and double diode models of three solar cells are considered for parameter optimization. The comparative error analysis for single and double diode models

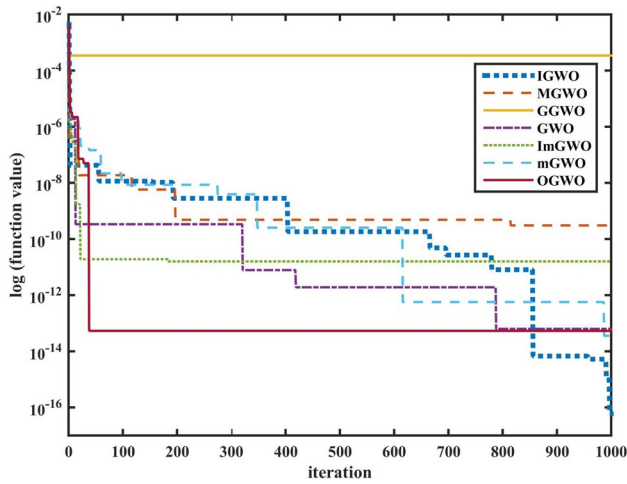
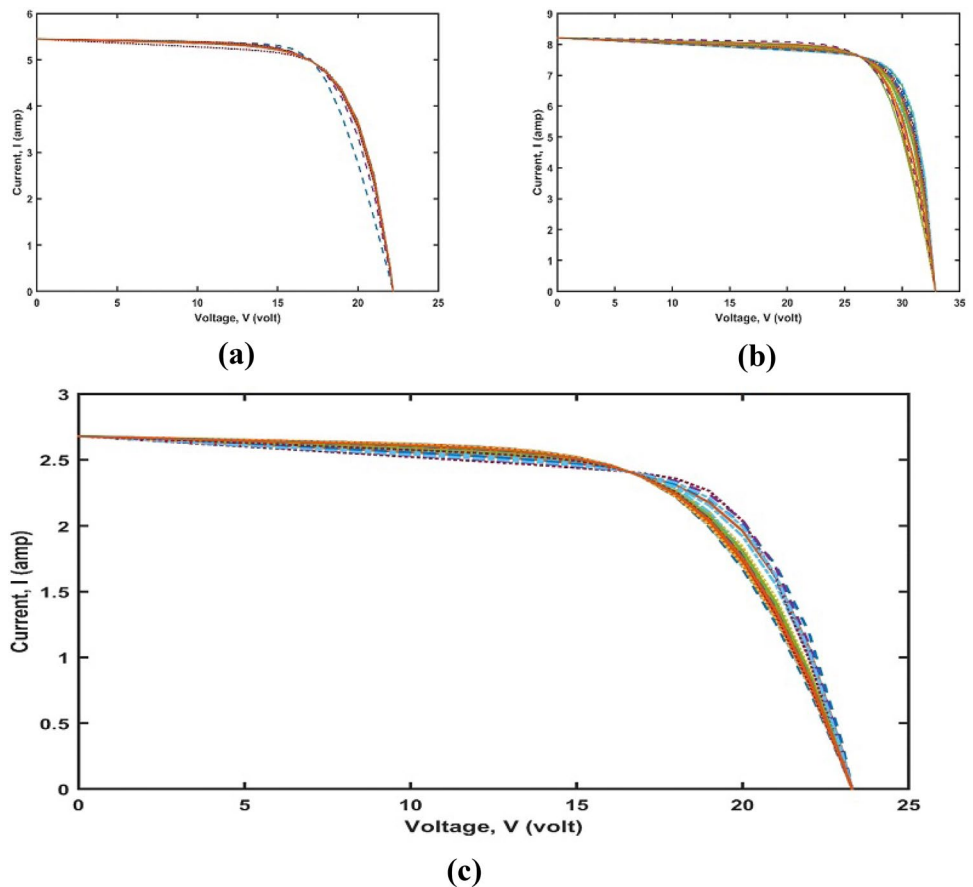


**Fig. 15** Thin-film convergence curve result comparison of double diode

are shown in Table 4. For single diode model mean and standard deviation values are optimal for all three PV cells, on the other hand for double diode model, polycrystalline cell has the optimal mean and standard deviation values.

**Fig. 16** I–V characteristics for **a** monocrystalline cell **b** polycrystalline cell **c** thin-film of double diode model



- For monocrystalline PV cell, mean value of double diode model is  $1.0760E - 11$  which is near to the best mean value of GWO i.e.  $8.1409E - 12$ . Similarly, for double diode thin film PV cell, mean value is  $1.0726E - 11$  which is close to the optimal solution of ImGWO i.e.  $9.5102E - 12$ . Hence for both PV cells results obtained using IGWO are comparable to results obtained using other methods.

### 5.3 Execution time analysis

As per Fig. 17, it can be easily seen that execution time of algorithms with IGWO is competitive. However, in the cases of internal loop chaotic algorithm takes more time. The execution time is calculated as the mean value of 30 independent runs of each algorithm and simulations are performed on intel Core (TM) i5-9400 cpu, 8 GB Ram computing machine. From the analysis it can be said that sinusoidal bridging and opposition based learning mechanism help IGWO to get acceleration in exploitation phase.

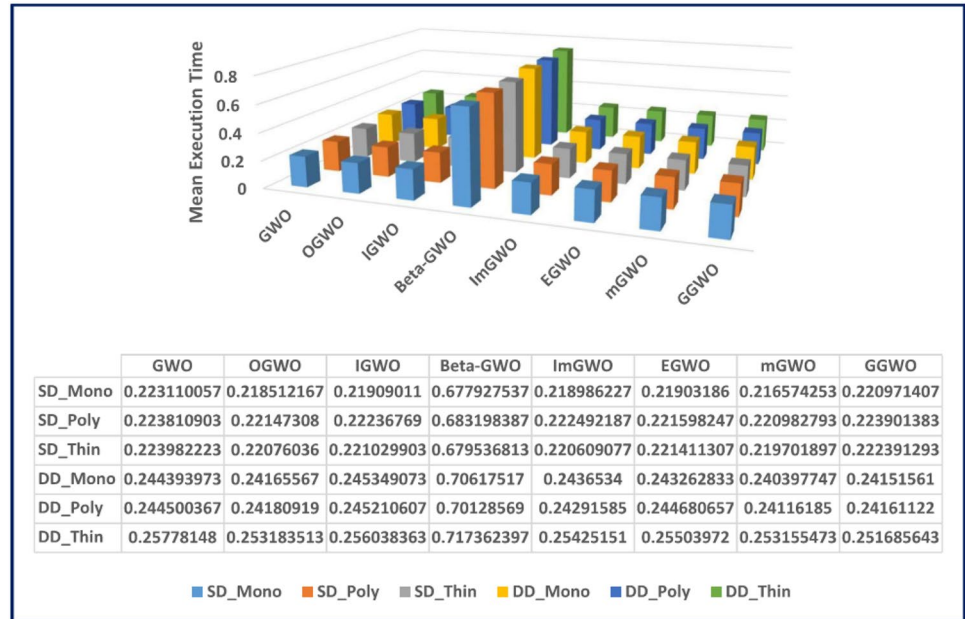
**Table 3** Parameters values for double diode model

Module	Parameters	IGWO [34]	MGWO [47]	GGWO [48]	ImGWO [49]	mGWO [50]	OGWO [51]	GWO [38]
Monocrystalline cell	$I_{rsc_1}$	4.35E-07	8.59E-08	5.42E-07	4.35E-07	3.84E-07	4.47E-07	3.11E-07
	$\psi_1$	1.80E+00	1.52E+00	1.76E+00	1.80E+00	1.88E+00	1.82E+00	1.74E+00
	$\psi_2$	1.41E+00	1.47E+00	1.29E+00	1.41E+00	1.64E+00	1.70E+00	1.56E+00
	$R_{SE}$	2.54E-01	9.14E-02	3.15E-01	2.54E-01	1.31E-01	9.97E-02	1.66E-01
	$R_{SH}$	1.07E+02	5.70E+01	1.30E+02	1.07E+02	1.08E+02	1.17E+02	1.05E+02
	$I_{rsc_2}$	2.80E-05	3.12E-06	2.97E-06	2.86E-06	1.56E-05	1.72E-05	1.25E-05
	$I_{dmc}$	5.45E+00	5.46E+00	5.46E+00	5.47E+00	5.46E+00	5.46E+00	5.46E+00
Polycrystalline cell	$I_{rsc_1}$	4.17E-07	8.40E-08	5.54E-07	3.58E-07	2.85E-07	3.58E-07	2.80E-07
	$\psi_1$	1.75E+00	1.39E+00	1.67E+00	1.82E+00	1.69E+00	1.77E+00	1.74E+00
	$\psi_2$	1.06E+00	7.21E-01	1.05E+00	1.15E+00	9.52E-01	9.92E-01	1.02E+00
	$R_{SE}$	9.12E-02	3.49E-02	2.05E-01	1.44E-01	1.32E-01	8.62E-02	9.65E-02
	$R_{SH}$	7.02E+01	5.05E+01	1.23E+02	1.06E+02	6.46E+01	5.83E+01	7.44E+01
	$I_{rsc}$	6.71E-08	6.26E-10	1.26E-06	1.43E-07	1.38E-07	3.80E-08	1.51E-07
	$I_{dmc}$	8.22E+00	8.22E+00	8.22E+00	8.22E+00	8.23E+00	8.22E+00	8.22E+00
Thin-Film	$I_{rsc_1}$	3.59E-07	2.73E-08	5.13E-07	4.21E-07	3.18E-07	4.33E-07	2.55E-07
	$\psi_1$	1.81E+00	1.60E+00	1.82E+00	1.92E+00	1.83E+00	1.90E+00	1.84E+00
	$\psi_2$	1.74E+00	8.77E-01	1.35E+00	1.47E+00	1.34E+00	1.52E+00	1.49E+00
	$R_{SE}$	7.01E-01	3.74E-03	5.63E-01	5.04E-01	5.60E-01	6.15E-01	4.04E-01
	$R_{SH}$	1.17E+02	6.21E+01	9.45E+01	9.29E+01	9.72E+01	1.02E+02	9.21E+01
	$I_{rsc_2}$	3.10E-06	7.08E-13	2.76E-06	1.96E-06	1.89E-06	2.60E-06	2.76E-06
	$I_{dmc}$	2.70E+00	2.68E+00	2.69E+00	2.69E+00	2.70E+00	2.70E+00	2.69E+00

**Table 4** Comparative analysis of error in objective function of representative models between IGWO and other variants of GWO

Model	Film		IGWO [34]	MGWO [47]	GGWO [48]	ImGWO [49]	mGWO [50]	OGWO [51]	GWO [38]
Single diode model	Monocrystal-line cell	min	<b>1.3827E-18</b>	5.3870E-14	5.0102E-11	1.2794E-14	2.0640E-17	9.6548E-17	2.1456E-17
		max	1.3833E-11	6.4374E-09	0.0085	7.5507E-10	1.9914E-10	5.5031E-11	5.1955E-11
		SD	<b>2.5246E-12</b>	1.3157E-09	0.0021	2.3290E-10	4.4816E-11	1.0779E-11	1.0136E-11
		mean	<b>4.6577E-13</b>	5.3458E-10	9.7508E-04	1.6809E-10	2.0989E-11	4.0056E-12	3.6989E-12
	Polycrystalline cell	min	<b>3.0655E-17</b>	6.2376E-14	1.6943E-10	5.9181E-14	2.7119E-15	7.4821E-17	2.0254E-14
		max	2.3482E-10	3.3927E-10	0.0119	6.7459E-10	1.1632E-10	4.8284E-11	6.0949E-11
		SD	<b>4.2902E-11</b>	8.4670E-11	0.0029	1.6773E-10	2.3376E-11	1.2833E-11	1.4594E-11
		mean	<b>8.5081E-12</b>	6.7608E-11	0.0021	1.1501E-10	1.5271E-11	7.0701E-12	8.2839E-12
	Thin-film	min	<b>1.2928E-18</b>	1.1140E-13	3.8171E-12	7.8458E-15	4.8692E-17	8.7142E-15	1.9483E-18
		max	1.9272E-13	2.8918E-10	1.9288E-05	5.0004E-11	3.6197E-11	1.2293E-11	1.0280E-10
		SD	<b>3.5083E-14</b>	7.2970E-11	3.5190E-06	1.6090E-11	7.1846E-12	2.6783E-12	1.8725E-11
		mean	<b>7.0430E-15</b>	4.7130E-11	6.5825E-07	9.1491E-12	4.5106E-12	1.5765E-12	4.4487E-12
Double diode model	Monocrystal-line cell	min	<b>5.1141E-20</b>	3.8033E-15	2.0824E-11	1.4730E-13	9.0931E-15	2.3259E-17	3.5892E-15
		max	3.2044E-10	6.0611E-09	0.0453	1.8564E-09	1.3803E10	7.8672E-11	7.2367E-11
		SD	5.8490E-11	1.1467E-09	0.0105	3.5025E-10	3.5775E-11	<b>4.2973E-12</b>	1.7774E-11
		mean	1.0760E-11	4.4851E-10	0.0068	1.6510E-10	2.5077E-11	1.4385E-11	<b>8.1409E-12</b>
	Polycrystalline cell	min	<b>3.4908E-18</b>	1.9216E-15	2.0704E-07	1.0987E-14	1.0302E-15	2.1267E-15	5.1184E-16
		max	3.8653E-11	1.1936E-09	0.4623	1.4370E09	9.0782E-10	1.1911E-10	2.6508E-10
		SD	<b>7.8094E-12</b>	2.3682E-10	0.0921	4.5026E-10	1.9313E-10	2.6857E-11	5.6392E11
		mean	<b>1.9534E-12</b>	1.0090E-10	0.0335	3.1595E-10	8.5987E-11	1.0512E-11	2.3053E-11
	Thin-film	min	<b>3.6430E-20</b>	1.6733E-15	1.2418E-13	2.4157E-14	1.0151E-16	3.1960E-15	4.3486E-16
		max	3.2139E-10	1.0147E-09	0.0045	7.5579E-11	3.7636E-11	4.5269E-11	1.4580E-11
		SD	5.8674E-11	3.0123E-10	0.0010	1.5904E-11	7.2943E-12	<b>8.4502E-12</b>	2.8632E-12
		mean	1.0726E-11	1.7153E-10	6.0869E-04	<b>9.5102E-12</b>	3.9466E-12	2.9128E-12	1.3465E-12

Fig. 17 Execution time analysis



### 5.4 Validation of the results: statistical methods

It is quite empirical to state that metaheuristic algorithms possess randomness in nature and hence, the clear interpretation can't be drawn from the results of independent runs. It may be possible that for one instance particular algorithm gives better results and in next instances it fails. In such situations, various statistical tests can be conducted. In this section results of those statistical tests are presented that includes Wilcoxon Rank-sum test.

Results of Wilcoxon Rank-sum test has been depicted in Table 5. The column entries of table are the *p* values associated with the rank-sum test when competitor algorithm is compared with IGWO. Results of independent runs (30) are stored in an array for each algorithm and compared separately with the results of IGWO. *p* values less than 0.05 indicates that a significant difference exists between compared algorithm and IGWO, hence, it can be said that if IGWO is performing better in one set of runs in an optimization

process it will produce same results and outperforms the competitor for another sets of optimization process. We observed that the *p* values for this test are less than 0.05 for both representative models and for all algorithms.

SD(Mono), SD(Poly) SD(Thin) are the results of representative models single diode realization with Monocrystalline, Polycrystalline and thin films. The same is applicable for double diode representative models. *p* values that favors IGWO optimization efficacy are depicted in bold face. Further, the t test has also been conducted for the competitor algorithms.

Table 6 presents paired sample t test where a comparison between the results of independent runs of IGWO is carried out with other algorithms, the null hypothesis is that both the algorithms produces results that have normal distribution with mean equal to zero and unknown variance. The results where the *p* values are less than 0.05 and H values 1 are affirmative cases where a clear distinction can be obtained between IGWO and other variants.

Table 5 Comparative rank-sum analysis algorithms for extraction of single and double diode models

Representative model	$\beta$ -GWO	MGWO	GGWO	ImGWO	mGWO	OGWO
SD_Mono	<b>9.26E-09</b>	<b>6.07E-11</b>	<b>3.02E-11</b>	<b>8.99E-11</b>	<b>8.48E-09</b>	<b>1.07E-07</b>
SD_Poly	<b>1.31E-08</b>	<b>1.41E-09</b>	<b>3.34E-11</b>	<b>1.29E-09</b>	<b>1.85E-08</b>	<b>4.94E-05</b>
SD_Thin	<b>7.38E-10</b>	<b>4.08E-11</b>	<b>3.02E-11</b>	<b>6.70E-11</b>	<b>4.62E-10</b>	<b>9.92E-11</b>
Representative model	$\beta$ -GWO	MGWO	GGWO	ImGWO	mGWO	OGWO
DD_Mono	<b>8.48E-09</b>	<b>6.72E-10</b>	<b>3.69E-11</b>	<b>6.72E-10</b>	<b>3.50E-09</b>	<b>4.80E-07</b>
DD_Poly	<b>5.09E-08</b>	<b>3.82E-09</b>	<b>3.02E-11</b>	<b>3.82E-10</b>	<b>3.82E-09</b>	<b>5.53E-08</b>
DD_Thin	<b>1.56E-08</b>	<b>6.12E-10</b>	<b>5.49E-11</b>	<b>8.89E-10</b>	<b>4.57E-09</b>	<b>3.20E-09</b>

**Table 6** Comparative analysis of algorithms for t-test

Representative model	SD_Mono		SD_Poly		SD_Thin	
	H value	P value	H value	P value	H value	P value
$\beta$ -GWO	<b>1.00E+00</b>	<b>1.86E-02</b>	0.00E+00	6.74E-01	<b>1.00E+00</b>	<b>5.72E-04</b>
DGWO	<b>1.00E+00</b>	<b>3.42E-02</b>	<b>1.00E+00</b>	<b>2.12E-04</b>	<b>1.00E+00</b>	<b>1.38E-03</b>
GGWO	<b>1.00E+00</b>	<b>1.59E-02</b>	<b>1.00E+00</b>	<b>3.60E-04</b>	0.00E+00	3.14E-01
ImGWO	<b>1.00E+00</b>	<b>4.72E-04</b>	<b>1.00E+00</b>	<b>2.83E-03</b>	<b>1.00E+00</b>	4.16E-03
mGWO	<b>1.00E+00</b>	<b>1.86E-02</b>	<b>0.00E+00</b>	4.29E-01	<b>1.00E+00</b>	<b>1.82E-03</b>
OGWO	0.00E+00	8.99E-02	0.00E+00	8.63E-01	<b>1.00E+00</b>	<b>3.28E-03</b>
Representative model	DD_Mono		DD_Poly		DD_Thin	
	H value	<i>p</i> value	H value	<i>p</i> value	H value	<i>p</i> value
$\beta$ -GWO	0.00E+00	6.64E-01	0.00E+00	6.00E-02	0.00E+00	3.65E-01
DGWO	<b>1.00E+00</b>	<b>4.62E-02</b>	<b>1.00E+00</b>	<b>3.02E-02</b>	<b>1.00E+00</b>	<b>8.44E-03</b>
GGWO	<b>1.00E+00</b>	<b>1.43E-03</b>	0.00E+00	5.57E-02	<b>1.00E+00</b>	<b>2.95E-03</b>
ImGWO	<b>1.00E+00</b>	<b>2.32E-02</b>	<b>1.00E+00</b>	<b>6.25E-04</b>	0.00E+00	9.11E-01
mGWO	0.00E+00	2.84E-01	<b>1.00E+00</b>	<b>2.44E-02</b>	0.00E+00	5.37E-01
OGWO	0.00E+00	5.66E-01	0.00E+00	1.13E-01	0.00E+00	4.77E-01

**Table 7** Comparative analysis of algorithms for t-test2

Representative model	SD_Mono		SD_Poly		SD_Thin	
	H value	<i>p</i> value	H value	<i>p</i> value	H value	<i>p</i> value
$\beta$ -GWO	<b>1.00E+00</b>	<b>1.29E-02</b>	0.00E+00	6.69E-01	<b>1.00E+00</b>	<b>2.80E-04</b>
DGWO	<b>1.00E+00</b>	<b>3.01E-02</b>	<b>1.00E+00</b>	<b>1.19E-03</b>	<b>1.00E+00</b>	<b>8.03E-04</b>
GGWO	<b>1.00E+00</b>	<b>1.31E-02</b>	<b>1.00E+00</b>	<b>1.60E-04</b>	0.00E+00	3.10E-01
ImGWO	<b>1.00E+00</b>	<b>2.20E-04</b>	<b>1.00E+00</b>	<b>1.34E-03</b>	<b>1.00E+00</b>	<b>2.88E-03</b>
mGWO	<b>1.00E+00</b>	<b>1.51E-02</b>	0.00E+00	4.51E-01	<b>1.00E+00</b>	<b>1.11E-03</b>
OGWO	0.00E+00	8.52E-02	0.00E+00	8.61E-01	<b>1.00E+00</b>	<b>2.17E-03</b>
Representative model	DD_Mono		DD_Poly		DD_Thin	
	H value	<i>p</i> value	H value	<i>p</i> value	H value	<i>p</i> value
$\beta$ -GWO	0.00E+00	6.58E-01	<b>1.00E+00</b>	<b>4.66E-02</b>	0.00E+00	3.60E-01
DGWO	<b>1.00E+00</b>	<b>4.12E-02</b>	<b>1.00E+00</b>	<b>2.59E-02</b>	<b>1.00E+00</b>	<b>5.72E-03</b>
GGWO	<b>1.00E+00</b>	<b>8.39E-04</b>	0.00E+00	5.09E-02	<b>1.00E+00</b>	<b>1.95E-03</b>
ImGWO	<b>1.00E+00</b>	<b>2.06E-02</b>	<b>1.00E+00</b>	<b>3.28E-04</b>	0.00E+00	9.13E-01
mGWO	0.00E+00	2.57E-01	<b>1.00E+00</b>	<b>2.06E-02</b>	0.00E+00	5.32E-01
OGWO	0.00E+00	5.59E-01	0.00E+00	9.91E-02	0.00E+00	4.73E-01

Table 7 presents analysis of ttest 2 (two sample t test) where the indicated two samples are the results accumulated by IGWO in different independent runs and competing samples are from different algorithms. Null hypothesis states that the data used in two samples come from independent random samples from normal distributions with equal means and equal but unknown variances, the results indicated in the table depicts the hypothesis value and p values of the test H values 1 and p values less than 0.05 are affirmative cases where IGWO is outperforming other algorithms.

## 6 Conclusion

This paper has proposed an application of a recently developed version of GWO termed as IGWO. Optimal extraction of parameters of solar cells has been done using experimental values of signature voltage and currents at three different crucial points of I–V characteristic of solar cells. Implementation details of the developed algorithm and its results obtained from optimization processes have been exhibited to show case supremacy of the developed version over some

recently developed version of GWO. Following are the noteworthy contributions of this manuscript:

1. An objective function that comprises minimum data sheet information based on only three operating conditions is employed and solved with the help of different optimizers for extracting the parameters of representative models of solar panel.
2. Three configurations of films have been considered to perform simulation studies. We observe that the performance of IGWO is satisfactory as compared with other optimizers.
3. The effectiveness of IGWO is shown by the convergence curve of error values of PV cells by using single and double diode model as compared to other variants. We observe that mechanism of opposition based learning as well as bridging through sinusoidal operator help the algorithm from local minima entrapment and provide a boost in convergence.
4. It has also been observed through execution time analysis that this accuracy is not compromised with the execution time as the execution time is competitive as compared with all competitors. Further, the statistical analyses in form of rank-sum test, ttest and sample ttest have also been included to showcase the optimization efficacy of the algorithm.

To extract parameter values of PV cells with new objective function by considering multiple points and testing of IGWO on more challenging problems like protein structure prediction, AGC regulator design and Model Order Reduction are kept for future scope.

## Compliance with ethical standards

**Conflict of interest** Authors of the manuscript declare that there is no conflict of interest regarding the publication of this paper.

## References

1. El-Naggar KM, AlRashidi MR, AlHajri MF, Al-Othman AK (2012) Simulated annealing algorithm for photovoltaic parameters identification. *Sol Energy* 86(1):266–274
2. AlHajri MF, El-Naggar KM, AlRashidi MR, Al-Othman AK (2012) Optimal extraction of solar cell parameters using pattern search. *Renew Energy* 44:238–245
3. Ishaque K, Salam Z, Mekhilef S, Shamsudin A (2012) Parameter extraction of solar photovoltaic modules using penalty-based differential evolution. *Appl Energy* 99:297–308
4. Askarzadeh A, Rezazadeh A (2013) Extraction of maximum power point in solar cells using bird mating optimizer-based parameters identification approach. *Sol Energy* 90:123–133
5. Gong W, Cai Z (2013) Parameter extraction of solar cell models using repaired adaptive differential evolution. *Sol Energy* 94:209–220
6. Jiang LL, Douglas LM, Jagdish CP (2013) Parameter estimation of solar cells and modules using an improved adaptive differential evolution algorithm. *Appl Energy* 112:185–193
7. Rajasekar N, Neeraja KK, Rini V (2013) Bacterial foraging algorithm based solar PV parameter estimation. *Sol Energy* 97:255–265
8. Bagher AM, Mirzaei MAV, Mirhabibi M (2015) Types of solar cells and application. *Am J Opt Photon* 3(5):94–113
9. Differences of Solar Cell Modules. <https://www.sempruis.com/comparing-mono-polycrystalline-and-thin-film-solar-panels/>
10. Arjyadhara P, Ali SM, Jena C (2013) Analysis of solar PV cell performance with changing irradiance and temperature. *Int J Eng Comput Sci* 2(1):214–220
11. Bai J, Liu S, Hao Y, Zhang Z, Jiang M, Zhang Yu (2014) Development of a new compound method to extract the five parameters of PV modules. *Energy Convers Manage* 79:294–303
12. Joshi AS, Dincer I, Reddy BV (2009) Performance analysis of photovoltaic systems: a review. *Renew Sustain Energy Rev* 13(8):1884–1897
13. Ma T, Yang H, Lin L (2013) Performance evaluation of a stand-alone photovoltaic system on an isolated island in Hong Kong. *Appl Energy* 112:663–672
14. Ghoneim AA (2006) Design optimization of photovoltaic powered water pumping systems. *Energy Convers Manage* 47(11–12):1449–1463
15. Jordehi AR (2016) Parameter estimation of solar photovoltaic (PV) cells: a review. *Renew Sustain Energy Rev* 61:354–371
16. Allam D, Yousri DA, Eteiba MB (2016) Parameters extraction of the three diode model for the multi-crystalline solar cell/module using Moth-Flame Optimization Algorithm. *Energy Convers Manage* 123:535–548
17. Nishioka K, Sakitani N, Uraoka Y, Fuyuki T (2007) Analysis of multicrystalline silicon solar cells by modified 3-diode equivalent circuit model taking leakage current through periphery into consideration. *Sol Energy Mater Sol Cells* 91(13):1222–1227
18. Ishaque K, Salam Z, Taheri H (2011) Simple, fast and accurate two-diode model for photovoltaic modules. *Sol Energy Mater Sol Cells* 95(2):586–594
19. Appelbaum J, Peled A (2014) Parameters extraction of solar cells: a comparative examination of three methods. *Sol Energy Mater Sol Cells* 122:164–173
20. Oliva D, Cuevas E, Pajares G (2014) Parameter identification of solar cells using artificial bee colony optimization. *Energy* 72:93–102
21. Alam DF, Yousri DA, Eteiba MB (2015) Flower pollination algorithm based solar PV parameter estimation. *Energy Convers Manage* 101:410–422
22. Chin VJ, Zainal S, Kashif I (2015) Cell modelling and model parameters estimation techniques for photovoltaic simulator application: A review. *Appl Energy* 154:500–519
23. Jamadi M, Merrikh-Bayat F, Bigdeli M (2016) Very accurate parameter estimation of single-and double-diode solar cell models using a modified artificial bee colony algorithm. *Int J Energy Environ Eng* 7(1):13–25
24. Xiong G, Zhang J, Shi D, He Y (2018) Parameter extraction of solar photovoltaic models using an improved whale optimization algorithm. *Energy Convers Manage* 174:388–405
25. Abd Elaziz M, Oliva D (2018) Parameter estimation of solar cells diode models by an improved opposition-based whale optimization algorithm. *Energy Convers Manage* 171:1843–1859
26. Biswas PP, P. N S, Guohua W, Gehan AJA (2019) Parameter estimation of solar cells using datasheet information with the



- application of an adaptive differential evolution algorithm. *Renew Energy* 132:425–438
27. Hassanien AE, Rizk-Allah RM, Elhoseny M (2018) A hybrid crow search algorithm based on rough searching scheme for solving engineering optimization problems. *J Ambient Intell Hum Comput* pp 1–25
  28. Rizk-Allah RM, Hassanien AE, Bhattacharyya S (2018) Chaotic crow search algorithm for fractional optimization problems. *Appl Soft Comput* 71:1161–1175
  29. Rizk-Allah RM, Hassanien AE (2018) New binary bat algorithm for solving 0–1 knapsack problem. *Complex Intell Syst* 4(1):31–53
  30. Rizk-Allah RM, Hassanien AE, Elhoseny M, Gunasekaran M (2019) A new binary salp swarm algorithm: development and application for optimization tasks. *Neural Comput Appl* 31(5):1641–1663
  31. Zhang Y, Gong DW, Sun XY, Geng N (2014) Adaptive bare-bones particle swarm optimization algorithm and its convergence analysis. *Soft Comput* 18(7):1337–1352
  32. Zhang Y, Gong DW, Ding Z (2012) A bare-bones multi-objective particle swarm optimization algorithm for environmental/economic dispatch. *Inf Sci* 192:213–227
  33. Zhang Y, Song XF, Gong DW (2017) A return-cost-based binary firefly algorithm for feature selection. *Inf Sci* 418:561–574
  34. Saxena A, Bhanu PS, Rajesh K, Vikas G (2018) Intelligent Grey Wolf Optimizer Development and application for strategic bidding in uniform price spot energy market. *Appl Soft Comput* 69:1–13
  35. Villalva MG, Jonas RG, Ernesto RF (2009) Comprehensive approach to modeling and simulation of photovoltaic arrays. *IEEE Trans Power Electron* 24(5):1198–1208
  36. Soon JJ, Kay-Soon L (2012) Photovoltaic model identification using particle swarm optimization with inverse barrier constraint. *IEEE Trans Power Electron* 27(9):3975–3983
  37. KC200GT High Efficiency Multicrystal Photovoltaic Module Datasheet Kyocera. <http://www.kyocerasolar.com/asset/s/001/5195.pdf>
  38. Mirjalili S, Seyed MM, Andrew L (2014) Grey wolf optimizer. *Adv Eng Softw* 69:46–61
  39. Emary E, Hossam MZ, Aboul EH (2016) Binary grey wolf optimization approaches for feature selection. *Neurocomputing* 172:371–381
  40. Gupta E, Saxena A (2016) Grey wolf optimizer based regulator design for automatic generation control of interconnected power system. *Cogent Eng* 3(1):1151612
  41. Saxena A, Shekhawat S. (2017). Ambient air quality classification by grey wolf optimizer based support vector machine. *J Environ Public Health*
  42. Tizhoosh HR (2005) Opposition-based learning: a new scheme for machine intelligence. In: International conference on computational intelligence for modelling, control and automation and international conference on intelligent agents, web technologies and internet commerce (CIMCA-IAWTIC'06), vol 1, pp 695–701. IEEE
  43. Shekhawat S, Saxena A (2020) Development and applications of an intelligent crow search algorithm based on opposition based learning. *ISA Trans* 99:210–230
  44. Saxena A (2019) A comprehensive study of chaos embedded bridging mechanisms and crossover operators for grasshopper optimisation algorithm. *Expert Syst Appl* 132:166–188
  45. Saxena A, Kumar R, Das S (2019) chaotic map enabled grey wolf optimizer. *Appl Soft Comput* 75:84–105
  46. Dinkar SK, Deep K (2017) Opposition based Laplacian ant lion optimizer. *J Comput Sci* 23:71–90
  47. Khandelwal A, Bhargava A, Sharma A, Sharma H (2018) Modified grey wolf optimization algorithm for transmission network expansion planning problem. *Arab J Sci Eng* 43(6):2899–2908
  48. Yang B, Zhang X, Tao Yu, Shu H, Fang Z (2017) Grouped grey wolf optimizer for maximum power point tracking of doubly-fed induction generator based wind turbine. *Energy Convers Manage* 133:427–443
  49. Madhilarasan M, Deepa SN (2016) Long-term wind speed forecasting using spiking neural network optimized by improved modified grey wolf optimization algorithm. *Int J Adv Res* 4(7):356–368
  50. Mittal N, Urvinder S, Balwinder SS (2016) Modified grey wolf optimizer for global engineering optimization. *Appl Comput Intell Soft Comput* 8
  51. Pradhan M, Provas KR, Tandra P (2017) Oppositional based grey wolf optimization algorithm for economic dispatch problem of power system. *Ain Shams Eng J* 9:2015–2025

**Publisher's Note** Springer Nature remains neutral with regard to jurisdictional claims in published maps and institutional affiliations.